

Fabrication of a fully integrated passive module for filter application using MCM-D compatible processes

SWAPAN K. BHATTACHARYA, JAE Y. PARK, RAG R. TUMMALA, MARK G. ALLEN *Packaging Research Center, School of Electrical and Computer Engineering, Georgia Institute of Technology, 813 Ferst Drive, Atlanta, GA 30332-0560, USA*
E-mail: swapan@ee.gatech.edu

Integral passive is an emerging technology which is currently perceived as a possible alternative to the discrete passive technology in fulfilling the next generation packaging needs. Although discrete surface mount passive components (resistors, capacitors, and inductors) have been well characterized, the development of integral passive components suitable for co-integration on the board level is relatively recent. Since in some applications the number of passive components can exceed the number and the area of IC chips on a circuit board or in a package, such integration of passive components would be necessary to substantially eliminate part count and reduce device area. To address these issues, integration technology for passive elements in the same manner as for transistors is necessary. In addition, the fabrication sequence of all integral passive components should be mutually compatible for co-integration on the same substrate. In this paper, materials and

fabrication issues for passive elements such as resistors (R), capacitors (C), and inductors (I) and the feasibility of integration of these fabricated passive components on glass substrates have been addressed. An active filter circuit has been selected for a case study for R, L, and C co-integration. This passive module contains eleven resistors, four capacitors, and four inductors, and is fabricated using MCM-D (multichip module-deposited) compatible processes. A variety of materials appropriate for fabrication of integral passives in a mutually compatible fashion were investigated, including chromium and nickel-chromium resistors, composites of high dielectric constant materials in epoxies for capacitor dielectrics, and composites of magnetic ferrite particles in polyimides for inductor core and shielding. The fabricated devices showed good agreement between the design values and the corresponding measured values. It is anticipated that some of these materials and fabrication processes can be implemented for the MCM-L (multichip module-laminate) compatible packaging.

~ 2000 Kluwer Academic Publishers

1. Introduction

Electronic industries are responding to the increasing consumer demand in telecommunications, computer, automotive, and consumer sectors for product miniaturization with progressively decreasing costs. However, miniaturization also requires an alternative technology such as integral passives that can potentially save significant real estate on the substrate. Although, integral passive technology has been perceived to be a viable option, there are several barriers in implementing this technology to reality. Some of these inhibitors are efficient circuit design with increased component density, qualification of new materials for passive components and substrates, cost, time-to-market, technology transfer, and product scale-up toward commercialization. The worldwide market in passive components is estimated to be \$25 billion today. This is projected from the fact

that according to the NEMI Roadmap, 900 billion parts were shipped worldwide in 1997. A cost of \$0.02 per part reflects a \$18B annual market [1].

Electronics products such as VCRs, camcorders, television tuners, and other communication devices utilize a large number of passive components. To meet higher component needs, many miniaturized discrete surface mount passive components (resistors, capacitors, and inductors) have been mounted on boards and modules in a hybrid fashion. Such surface mounting introduces additional expense of manufacture, large board area, and additional parasitics into the system thus limiting the system performance. These issues can be dealt with by integrating these passive components directly into a multichip module (MCM) substrate along with other IC chips [2]. The size of the board can be reduced (especially if chips can be placed above the

Report Documentation Page

Form Approved
OMB No. 0704-0188

Public reporting burden for the collection of information is estimated to average 1 hour per response, including the time for reviewing instructions, searching existing data sources, gathering and maintaining the data needed, and completing and reviewing the collection of information. Send comments regarding this burden estimate or any other aspect of this collection of information, including suggestions for reducing this burden, to Washington Headquarters Services, Directorate for Information Operations and Reports, 1215 Jefferson Davis Highway, Suite 1204, Arlington VA 22202-4302. Respondents should be aware that notwithstanding any other provision of law, no person shall be subject to a penalty for failing to comply with a collection of information if it does not display a currently valid OMB control number.

| | | | | | |
|---|------------------------------------|-------------------------------------|----------------------------|---|---------------------------------|
| 1. REPORT DATE 2000 | | 2. REPORT TYPE | | 3. DATES COVERED 00-00-2000 to 00-00-2000 | |
| 4. TITLE AND SUBTITLE Fabrication of a fully integrated passive module for filter application using MCM-D compatible processes | | | | 5a. CONTRACT NUMBER | |
| | | | | 5b. GRANT NUMBER | |
| | | | | 5c. PROGRAM ELEMENT NUMBER | |
| 6. AUTHOR(S) | | | | 5d. PROJECT NUMBER | |
| | | | | 5e. TASK NUMBER | |
| | | | | 5f. WORK UNIT NUMBER | |
| 7. PERFORMING ORGANIZATION NAME(S) AND ADDRESS(ES) Georgia Institute of Technology, School of Electrical and Computer Engineering, Atlanta, GA, 30332 | | | | 8. PERFORMING ORGANIZATION REPORT NUMBER | |
| 9. SPONSORING/MONITORING AGENCY NAME(S) AND ADDRESS(ES) | | | | 10. SPONSOR/MONITOR'S ACRONYM(S) | |
| | | | | 11. SPONSOR/MONITOR'S REPORT NUMBER(S) | |
| 12. DISTRIBUTION/AVAILABILITY STATEMENT Approved for public release; distribution unlimited | | | | | |
| 13. SUPPLEMENTARY NOTES | | | | | |
| 14. ABSTRACT | | | | | |
| 15. SUBJECT TERMS | | | | | |
| 16. SECURITY CLASSIFICATION OF: | | | 17. LIMITATION OF ABSTRACT | 18. NUMBER OF PAGES 6 | 19a. NAME OF RESPONSIBLE PERSON |
| a. REPORT unclassified | b. ABSTRACT unclassified | c. THIS PAGE unclassified | | | |

embedded passive components) and the parasitics associated with the passive components can also be reduced due to the elimination of leads and the shorter connections between passive components and other IC chips. Integration of passive elements can also result in reduced assembly costs, improved electrical performance, improved packaging efficiency, mass production by batch fabrication, low power loss, low volume, low weight, and low profile.

Much research has been done to realize integral passive components based on MCM-C (ceramic) and MCM-D (deposited) technology [3-5]. In these approaches, it is necessary to undergo high temperature fabrication such as in low temperature co-fired ceramics (LTCC) and high temperature co-fired ceramics (HTCC). In this paper, a fully integrated passive module is designed, fabricated, and characterized using MCM-D compatible and relatively low temperature (..., 300 °C) fabrication processes in order to test the feasibility of integration of passive components such as inductors, capacitors, and resistors. The passive module (dimension is 8mm x 10mm x 0.06mm) is fabricated with two lithography masks and one screen printing mask, and includes 11 integrated resistors (5-80.0.), 4 capacitors (14-160pF), and 4 inductors (145c.-650nH). The circuit schematic was provided by Bourns, Inc.

2. Design consideration

The capacitance (C) of a parallel plate metal-insulator-metal (MIM) capacitor is defined as follows:

$$C = \frac{\epsilon_0 \epsilon_r A}{d} \quad (1)$$

where ϵ_0 is dielectric constant of free space, ϵ_r is the dielectric constant of the capacitor dielectric material, A is the area of the effective electrode plates, and d is the distance between top and bottom plates. Polymer/ceramic composites have proven to be a favorable choice for thin film capacitors for the MCM-L technology [6-10]. These dielectric materials are two-phase composites in which the polymer allows low temperature fabrication and the filler enhances the dielectric constant of the resulting composite far beyond that of the unfilled polymer. However, there are many other requirements for integration of capacitors using thin film processes and screen printing which are adopted in the passive module fabrication described in this paper. Thin (5 μm) uniform films with higher dielectric constant (100 for most applications) and low loss ($\ll 0.01$), low temperature curing with high temperature stability, and good adhesion to metal substrate are of primary importance. Epoxy materials have been studied to evaluate the possibility of material cost reduction and their compatibility with the organic substrates.

Theoretically, the permittivity of the composites can be increased by selecting higher dielectric constant polymers and ceramics and maximizing the filler loading. The basic equation for permittivity of a two-phase composite system (E_r) is given by the Lichtenecker equation

$$E_r = V_1 \epsilon_1 + V_2 \epsilon_2 \quad (2)$$

where ϵ_1 and ϵ_2 are the permittivity of the individual phases, V_1 and V_2 are the respective volume fractions, and exponent n equals 1 or -1 for parallel and series connections, respectively [11,12]. This equation does not take into account the size and shape factors of the dispersed phase. Various modifications of this equation have been made to compare experimental data with the predicted values, the most accepted one for the filled polymer system being [13,14]:

$$\log E_r = \log(E_r^p) + (1 - K) v_f \log(E_r^f) \quad (3)$$

where K is a constant and depends on the filler and polymer systems, v_f is the volume fraction of filler, and E_r^p and E_r^f are the dielectric constants of the polymer and the filler, respectively. This modified equation has been previously utilized to calculate the dielectric constant of the two-phase composite and showed good agreement with the experimental values [6,7].

Integral resistors are designed based on rectangular cross-sections. Chromium metal was used as the resistive material due to the required low resistance values in this module. The resistance (R) of a rectangular resistor is defined as follows:

$$R = \frac{\rho l}{t w} \quad (4)$$

where ρ is the intrinsic resistivity, t is the thickness, l is the length, and w is the width of the rectangular resistor. For a particular process, l/w is defined as the number of "squares" in the resistor.

Integral inductors can be designed with different geometries such as spiral, meander, and bar type. Spiral type inductors are commonly used because of their simple geometries and ease of fabrication. NiZn ferrite is an appropriate core material for integral magnetic devices at higher frequencies due to its high resistivity and low dielectric constant. Polymer-filled NiZn ferrite is also used as a shielding material for high frequency operation. Shielding is required since integral inductors may be in closer proximity to other components than their hybrid-assembled counterparts. The integral inductors should also have compatible fabrication sequences with integral capacitors and resistors for application in multi-chip modules and other miniaturized electronic systems. The characteristics of integral inductors are strongly dependent on many parameters such as device structure, number of windings, conductor width/space sizes, device substrate, and the magnetic properties of the core. Integral inductors for this passive module were designed based on results from a variety of test structures [15-18].

3. Fabrication of the passive RLC module

The passive module (8 mm x 10mm x 0.06 mm thick) was fabricated with two lithography masks and one screen printing mask. The module includes 11 integrated resistors (5-80 Ω), 4 capacitors (14-160 pF), and 4 inductors (145-650 nH). Fig. 1 illustrates the filter circuit diagram. The component values are shown in Table I. The fabrication sequence is shown in fig. 2. A glass

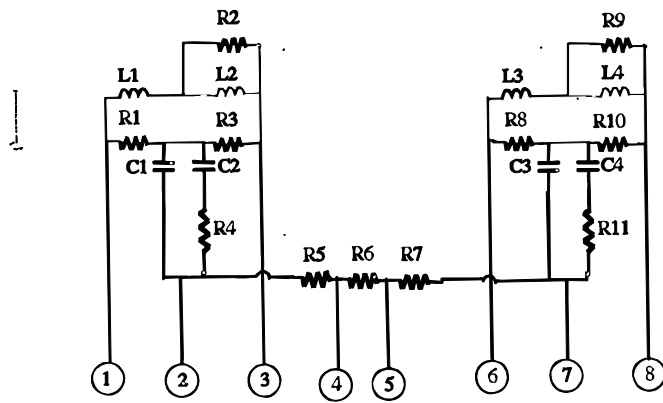


Figure 1 Electrical schematic of the Bourns filter circuit.

substrate was selected due to the ease of fabrication and for high temperature curing of polyimide.

3.1. Resistor lines

Chromium metal was selected as a resistive material due to the required low resistance in this module. Chromium was deposited by the evaporation technique. Meander type resistors were patterned on the glass substrate using photolithography and lift-off techniques. The important issue in the lift-off process is to create a mushroom-like resist mask. This resist mask prevents the metal evaporation on the side-wall of the resist and promotes dissolution of the resist pattern after the desired metal is deposited. Chlorobenzene was used to modify the surface dissolution characteristics of the photoresist mask. Shipley 1400-27 photoresist was spin-cast at 3000r.p.m. for 30s on a pre-cleaned glass substrate and soft-baked at 100°C for one minute on a hot plate. The photoresist was exposed through a patterned mask with 75 mJ cm⁻² at 240nm wavelength and subsequently dipped in chlorobenzene for 2 min. The sample was re-baked at 95 °C for 2min in a convention oven and developed using Microposit 354 developer for 20 to 30 s depending on the line width. Chromium metal was deposited on the patterned photoresist using an electron beam evaporator. The photoresist was released by dissolution in acetone. Fig. 3 shows a fabricated meander resistor pattern.

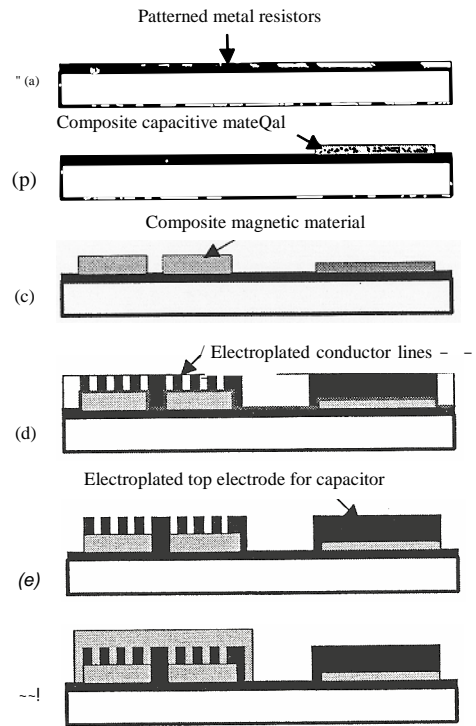


Figure 2 Fabrication sequences of the passives module: (a) formation of metal resistors; (b) deposition of capacitor material; (c) deposition of composite magnetic material; (d) electroplating of spiral type conductor lines, top electrode for capacitor, and interconnections of integral passives components; (e) removal of thick photoresist and bottom seed layer; (f) deposition of composite magnetic material on top of the spiral type conductor lines by screen printing.

3.2. Capacitors

The composite epoxy dielectric material was spun on top of the meander type metal resistors and patterned using standard lithography. Probimer-4959, a product of Ciba-Geigy, was selected for making small capacitor structures using lithographic techniques. This epoxy material has a dielectric constant of 3.5 and can be readily photodefined with good resolution. Finer particle size of the filler material (< 1 μm) is needed for casting thin films with a smooth surface to achieve higher specific capacitance. Lead magnesium niobate (average size of 1 μm) was selected as the filler material for its high dielectric constant value (~17 800 in the sintered form) and low loss (~0.015). Epoxy and cerami-

TAB LEI Comparison of designed and achieved values of integral passive components

| Passive components | Designed values (doc.) | Achieved values (100kHz) | Error rate (%) |
|--------------------|------------------------|--------------------------|----------------|
| R1, R3, R5, R10 | 75.0. | 68.Q | 9.3 |
| R2 | 19.1.0. | 16.5.Q | 13.6 |
| R4 | 294.0. | 275.Q | 6.4 |
| R5,R7 | 280.0. | 267.Q | 4.6 |
| R6 | 43.2.0. | 39.7.Q | 8.1 |
| R9 | 38.1.0. | 35.2.Q | 1.6 |
| R11 | 187.0. | 169.Q | 9.6 |
| C1 | 15pF | 14.5pF | 3.3 |
| C2 | 68pF | 71.2pF | 4.7 |
| C3 | 47pF | 49pF | 4.2 |
| C4 | 150pF | 156.2 pF | 4.1 |
| L1 | 0.111H | 0.145 | 4.5 |
| L2 | 0.39~ | 0.41 | 5.1 |
| L3 | 0.27~ | 0.256 | 5.2 |
| L4 | 0.8211H | 0.78 H | 4.8 |

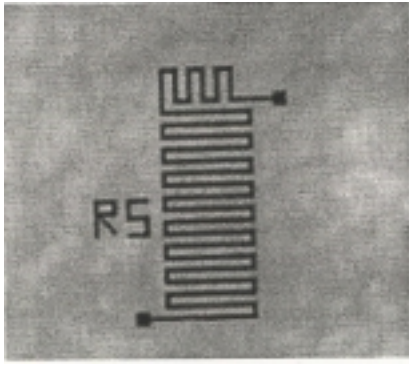


Figure 3 Photomicrograph of a meander type metal resistor.

powders were mixed in the required proportion (to yield 50 vol % filler in the composite) and blended using a Pro Scientific high shear homogenizer (Model PRO200). After mixing in the high shear apparatus, the coating solution was homogenized in a roll miller for 3 to 5 days prior to fabrication. This was done to prevent settling of the ceramic powder. The mixture was spin coated on glass substrates containing the chromium resistor lines at 2000 to 3000 r.p.m. for 60 to 90 s. The photodefinable epoxy was then baked on a hot plate to remove solvent, exposed to 320 nm UV radiation through a mask at 10mW power for 5 to 15min depending on the filler concentration. After UV exposure, samples were hard-baked to promote cross-linking in the exposed areas. These hard-baked samples were developed using an appropriate solvent to remove the uncross-linked domains and cured in an oven, at 150°C for 1h. Fig. 4 represents an example of the parallel plate capacitor fabricated at 50 vol % filler. The specific capacitance of the epoxy composite at 50 vol % was in the range 618 to 10nFcm⁻² at 100kHz.

3.3. Inductors

After curing the deposited epoxy capacitor layer, composite magnetic material was deposited selectively by screen printing. Photodefinable polyimide (PI 2721, DuPont) filled with magnetic ferrite particles served as the inductor core material. Composite magnetic material

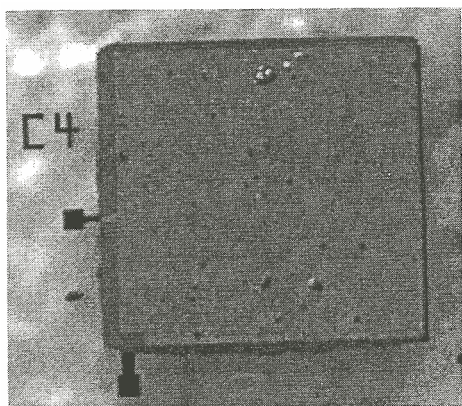


Figure 4 Photomicrograph of an epoxy composite capacitor. AhQ

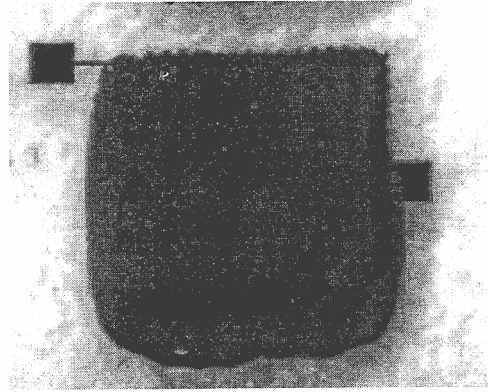


Figure 5 Photomicrograph of the integral microinductor incorporated in the RLC device.

was deposited on substrates by screen printing. The screen-printed material was cured at 200 to 300 °C. Titanium/copper/titanium layers were deposited using an electron beam evaporator to form a seed layer for electroplating. Thick photoresist was coated and molds were used to form spiral type conductor lines. After removing the top seed layer, copper was electroplated into the photoresist molds. The molds were removed by dissolution in acetone. The seed layer was wet-etched to isolate the conductor lines. For EM shielding, polymer-filled ferrite was screen printed on the top of electroplated copper conductor lines and between the conductor lines, and cured to remove solvents. Fig. 5 shows a photomicrograph of the integral polymer-filled ferrite inductor.

In the final step, a thin film of aluminum was deposited using d.c. sputtering. The metal was patterned and dry-etched in order to keep the resistors from being attacked in this process. Aluminum was etched at a rate of 0.1 μm min⁻¹ using plasma at 105W of incident power, 40 sccm of chlorine, and 66.6 Pa of base pressure. This gas mixture did not attack any other metal during the etching process. The fabricated samples were diced and tested.

Fig. 6 shows the photomicrograph of the fully integrated passive module prior to deposition of the magnetic composite material on the top and between the conductor lines. Fig. 7 shows the photomicrograph of the fully integrated passive module. The fabricated passive module is diced, tested, and simulated as shown in Fig. 8.

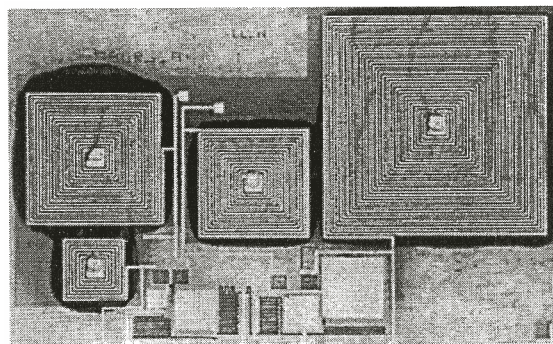


Figure 6 Photomicrograph of integrated passive module prior to deposition of polymer-filled ferrite on the top of spiral type conductor lines.

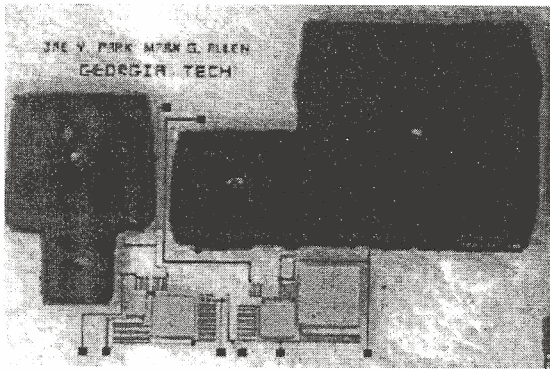


Figure 7 Photomicrograph of completed integrated passive module (11 resistors, 4 capacitors, and 4 inductors, dimension 8 mm x 10mm x 0.06mm)

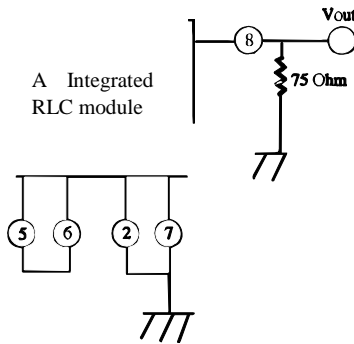


Figure 8 Test circuitry configuration of the integrated passive module.

Although this process is compatible with the MCM-D, it is expected that with proper selection of materials (such as epoxy instead of polyimide), it can be implemented in low temperature MCM-L compatible process~s.

4. Results and Discussions

The integrated resistors, capacitors, and inductors were characterized using a Hewlett-Packard impedance/gain-phase analyzer 4194A and a Kiethley LCZ meter. Table I compares designed and achieved values of embedded passive components. As shown in Table I, fabricated integral passive components are well matched with the designed values. In particular, capacitors and inductors have less than 5% error compared to the designed values. In order to gain an understanding of the operation of this module, a simulation using designed values of the passive components was compared with the simulated performance of the module using experimentally achieved component values (Table I) as well as their measured parasitics. Fig. 9 shows the output wave forms of the module circuits using designed and measured (with parasitics included) values when an a.c. pulse voltage with 2 ns rise and fall time, 10 ns delay time, and 11 ns width time is applied into the input terminal as shown in Fig. 8. Fig. 10 shows gain characteristics of the designed ideal circuit module and integrated real circuit module as a function of frequency. The integrated circuit has lower gain due to the stray capacitance and parasitic effects of the integral passive components at high

Figure 9 Comparison of an input wave form and output forms of the modules using designed and measured component values (with parasitics).

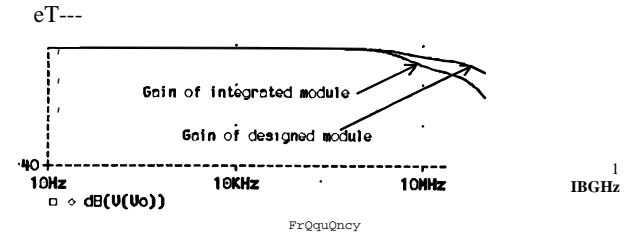


Figure 10 Comparison of gain of the module using designed and measured component values (with parasitics)

(a)

(b)

Figure 11 Comparison of output impedance of the module using designed and (b) measured component values (with parasitics).

frequencies. Fig. 11 shows the output impedance characteristics of the module using designed and measured values. In particular, the stray capacitance of integrated inductors causes lower resonant frequency in the integrated module compared with the designed circuit module.

5. Conclusions

A fully integrated passive module comprised of 11 resistors, 4 capacitors, and 4 inductors has been fabricated using MCM-D compatible processes. This prototype test vehicle demonstrated the feasibility of integration of passive components into the package or onto a silicon substrate. A variety of materials appropriate for fabrication of integral passives in a mutually compatible fashion were investigated, including chromium and nickel-chromium resistors, composites of high dielectric constant materials in epoxies for capacitor dielectrics, and composites of magnetic ferrite particles in polyimides for inductor core and shielding. The

fabricated RLC devices showed good agreement between the design values and the corresponding measured values of the individual passive components.

Acknowledgments

This work is supported in part by the DARPA Embedded Passives Consortium, Contract F33615-96-2-1838 and by the National Science Foundation through the Georgia Tech/NSF Engineering Research Center in Electronic Packaging (contract EEC-9402723).

References

1. J. RECTOR, Proceedings of the Forty-Eighth IEEE Electronic Component and Technology Conference (1997) 218.
2. J. PARK and M. ALLEN, IEEE Seventh Joint MMM-Intermag Conference, California (1998).
3. R. FRYE, K. TAI, M. LAU and A. LIN, Proceedings of the 1992 International Electronics Packaging Conference, 1 (1992), 343.
4. R. BROWN, A. SHAPIRO and P. POLINSKI, *Int. J. Microcircuits Packag.* 16 (1993) 328.
5. P. MCCAFFREY, Proceedings of the International Electronics Packaging Conference (1990) 411.
6. P. CHAHAL, R. TUMMALA and M. ALLEN, Proceedings of the International Society for Hybrid Microelectronics (1996) 126.
7. S. K. BHATTACHARYA, R. R. TUMMALA, P. CHAHAL and G. WHITE., Third International Conference on Advanced Packaging Materials, Braselton, GA (March 1997) 68.
8. D. K. DAS-GUPTA and K. DOUGHTY *Thin Solid Films* 158 (1998) 93.
9. P. CHAHAL, R. TUMMALA, M. ALLEN and M. SWAMINATHAN, *IEEE Trans. Compon. Packag. Manuf. Technol., Part B* 21 (1998) 184.
10. S. BHATTACHARYA and R. TUMMALA, 1: *Mater. Sci.; Mater. Electron.* (to appear).
11. K. LICHTENECKER, *Z. Phys.*, 10 (1909) 1005.
12. B. TAREEV, "Physics of Dielectric Materials", (Mir Publishers, Moscow, 1979) p. 116.
13. K. MAZUR, PhD thesis, Silesian University, Katowice, Poland (1968).
14. K. MAZUR in "Ferroelectric Polymers," Ch. 11, edited by H. S. Nalwa (Marcel Dekker, 1995).
15. J. PARK and M. ALLEN, Twelfth IEEE Applied Power Electronic Conference (1997) 361.
16. J. PARK, L. LARGORCE and M. ALLEN, IEEE International Magnetic Conference, ED-06, 1997.
17. J. PARK, PhD thesis, Georgia Institute of Technology (1998).
18. J. PARK, S. BHATTACHARYA and M. ALLEN, IMAPS International Symposium on Microelectronics, Philadelphia (1997) 59.

Received 21 March
and accepted 12 May 2000